

Characterization of High Current RRP[®] Wires as a Function of Magnetic Field, Temperature and Strain

A. Godeke, M. G. T. Mentink, D. R. Dietderich, and A. den Ouden

Abstract—A new instrument for the characterization of superconducting materials as a function of Magnetic Field, Temperature and Strain, was designed, constructed and tested at Lawrence Berkeley National Laboratory (LBNL). A U-shaped bending spring was selected, since that design has proven to enable accurate characterizations of a multitude of superconducting materials for more than a decade. The new device is validated through measurements on very high current Rod Restack Processed (RRP[®]) Internal-Tin (IT) wires, for which we will present initial results, including parameterizations of the superconducting phase boundaries and comparisons with other wire types. Accurate parametrization of modern high magnetic field conductors is important for the analysis of the performance of magnet systems.

Index Terms—Critical Current, Magnetic Field, Temperature, Strain, Nb₃Sn wires

I. INTRODUCTION

THE strain dependence of the superconducting properties of Nb₃Sn wires plays an important role in the material's application in magnets. The relevant intermetallic Niobium-Tin (A15) phase in wires is stable from about 18 to 25 at.% Sn, and the properties increase significantly when approaching stoichiometry [1]. The increase in current density (J_c) by a factor two in RRP[®] IT wire, manufactured by Oxford Superconducting Technology, Carteret, NJ (OST), was for a significant part a result of bringing the A15 in the wires close to stoichiometry [2]. It is suggested elsewhere, that strain dependence could depend on Sn content in the A15 [1]. On one hand, it can be argued that Sn rich A15 is in a higher degree of ordering than Sn poor A15, which could make the relative effect of introduction disorder through strain larger in Sn rich A15. On the other hand, Sn enrichment will increase the compositionally averaged upper critical magnetic field (H_{c2}^*), resulting in a reduced strain dependence of the critical current (I_c) at a given operating magnetic field H [3]. It is therefore important to investigate the strain dependence of high J_c RRP[®] wires and compare the results with the strain dependence of other wire types.

To study the effect of strain on wires, we duplicated at LBNL a variable temperature Ti-6Al-4V U-shaped bending

Manuscript received August 26, 2008. This work was supported by the Director, Office of Science, High Energy Physics, U.S. Department of Energy under contract No. DE-AC02-05CH11231.

A. Godeke (corresponding author; phone: +1-510-486-4356; e-mail: agodeke@lbl.gov) and D. R. Dietderich are with Lawrence Berkeley National Laboratory, Berkeley CA 94720, USA

M. G. T. Mentink and A. den Ouden are with the Low Temperature Division, Faculty of Science and Technology, University of Twente, P.O. Box 217, 7500 AE, Enschede, The Netherlands

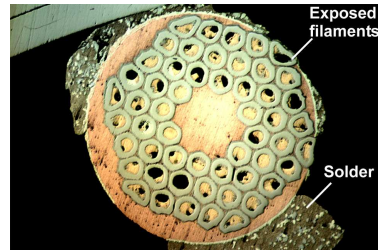


Fig. 1. Partially dissolved matrix Cu in a wire after measurement.

spring, which was developed at the University of Twente, Enschede, The Netherlands (UT) in 1996. The device at LBNL is an exact copy of the UT bending spring, which is extensively described elsewhere [4], [5]. The U-shaped bending spring has a relatively simple layout, with a small thermal mass that allows for rapid temperature control and compensation for power dissipation in the sample, and relatively simple operation. In addition, it has a flat surface perpendicular to the applied magnetic field that allows for the more fundamental analysis of simplified structures such as bulk materials and thin films. A disadvantage is the limited sample length of 45 mm which leads, through current redistribution effects, to an effective voltage tap length around 5 mm. The advantages, however, when recognized, outweigh the disadvantages. This paper describes initial measurements of modern OST high J_c RRP[®] wires.

II. SAMPLE AND PREPARATION

Three OST-RRP[®] wires, from billets 8781, 8857, and 9362, similar to wires used in the U.S. Large Hadron Collider Accelerator Research Program (LARP) with a nominal $J_c(12\text{ T}, 4.2\text{ K}) = 3\text{ kA/mm}^2$, were heat treated on reaction holders according to the LARP standard heat treatment, with a peak Nb₃Sn formation temperature of 640°C for 48 hours. The samples below are identified by their billet numbers. It should be emphasized that the LARP heat treatment results in an under-reaction to retain a high Residual Resistive Ratio (RRR) in Rutherford cables, at the cost of a small reduction in the critical properties [2], [6]. The reacted wires are transferred to the U-shaped bending spring and soldered to the bending spring with Sn-3.5wt.% Ag.

During the measurements, it became evident that samples 8781, 8857, and 9362 showed initial I_c values that were reduced by 15%, 20%, and 40%, respectively, compared to wires on standard Ti-6Al-4V I_c barrels, whereas an increased

TABLE I

COMPARISON OF THE MELT TEMPERATURE (T_{melt}), AND ROOM TEMPERATURE YIELD STRESS (σ_{yield}), YOUNG'S MODULES (E), AND YIELD STRAIN (ϵ_{yield}), FOR VARIOUS SOLDERING MATERIALS.

Material	T_{melt} [°C]	σ_{yield} [MPa]	E [GPa]	ϵ_{yield} [%]
Sn-3.5wt.% Ag	221	23	26	0.08
Sn-37wt.% Pb	183	27	16	0.17
Sn-58wt.% Bi	138	49	12	0.41

initial I_c has to be expected as a result of a smaller thermal pre-strain in wires mounted on the bending spring compared to I_c barrels [7]. The lowered initial I_c is indicative of sample damage during wire mounting, partly attributed to sticking of the wires to the reaction holders, and partly attributed to soldering at too high a temperature for too long.

The effect of the latter is illustrated by the cross-section after measurement of one of the samples, given in Fig. 1. From the Cu-Sn phase diagram it is clear that Cu dissolves into Sn above a temperature of 232°C, indicating that soldering should preferably be performed at a lower temperature, or the time at temperatures above 232°C has to be limited to prevent too much matrix Cu to dissolve into the solder. Fig. 1 indicates that, at least for this wire, this was clearly not the case, as is evident from the amount of matrix Cu that disappeared, thereby exposing the sub-elements. Table I provides a comparison of the melt temperature and room temperature mechanical properties of three common types of solder. It is clear that Sn-3.5wt.% Ag is, with hindsight, the worst choice, and that common eutectic Sn-37wt.% Pb is a better choice, even though Pb is poisonous and superconducting below 0.5 T. The best choice found for our purpose is Sn-58wt.% Bi, which has a significantly higher yield strain (relevant for strain transfer to the sample) and a substantially lower melting point.

III. TYPICAL RESULTS

Even though the samples exhibited an initially reduced I_c , it was decided to perform measurements on the samples for the commissioning of the new instrument. An electric field criterion of $E_c = 5 \times 10^{-5}$ V/m was applied for the I_c determination. This is slightly higher than the common $E_c = 10^{-5}$ V/m criterion for Nb₃Sn I_c measurements, as a result of the limited sample length. $E_c = 5 \times 10^{-5}$ V/m was selected to avoid non-linearities at higher currents, resulting from current redistribution, from interfering with the I_c determinations.

A typical result, in the form of a ‘Kramer’ plot (i.e. $I^{0.5}(\mu_0 H)^{0.25}$ as a function of H) at constant temperatures, is depicted in Fig. 2. For sample 9362 temperatures from 4.2 to 12 K were measured and sample 8857 was used to analyze the tail in the Kramer plot, which is representative for a large compositional distribution in these under-reacted wires [8].

A measurement of the I_c as a function of axial strain (ϵ) at 15 T and 4.2 K is shown in Fig. 3. It is seen that the compressive strain region is reversible. A slight increase in I_c is observed after returning to the cooldown axial strain state, which could be an indication of a relaxation of the

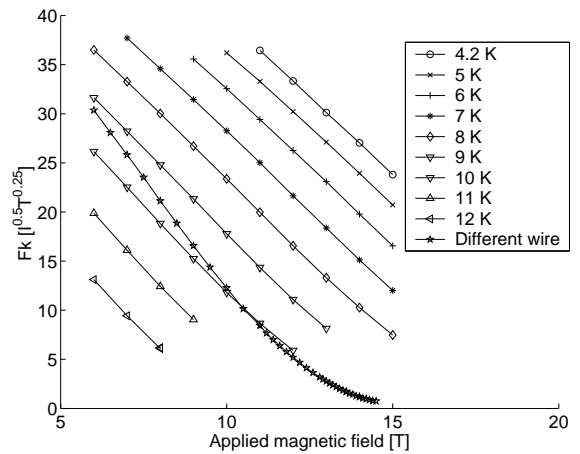


Fig. 2. Kramer plot at zero applied strain of $I_c(H)$ results at constant temperatures on sample 9362. One Kramer plot at 10 K, indicated by \star , was measured on sample 8857.

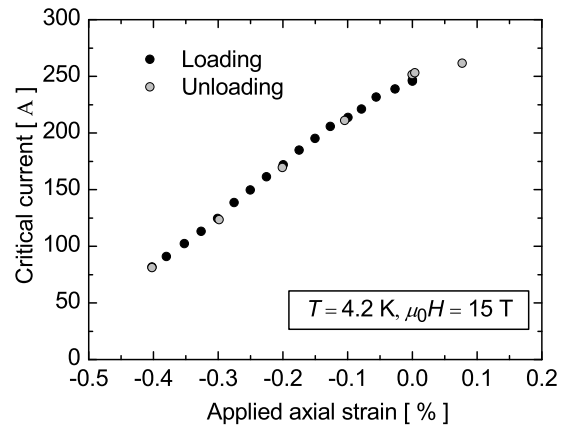


Fig. 3. Critical current as a function of applied axial strain at $\mu_0 H = 15$ T and $T = 4.2$ K on sample 8781.

three dimensional strain state in the A15 as a result of plastic deformations in the compressive strain region.

To accurately determine the maximum in the $I_c(\epsilon)$ dependence, a constant current of 270 A was used at $\mu_0 H = 15$ T and $T = 4.2$ K to provide sufficient voltage in the transition for an electric field $E \cong 90 \mu\text{Vm}^{-1}$. The axial strain was then increased in steps while recording $E(\epsilon)$. The results are shown in Fig. 4. Jumps in $E(\epsilon)$ appear just above 0.07% applied strain, and before the maximum superconducting properties are reached. When lowering the strain it is seen that the increase in voltage is irreversible, which is indicative of crack formation inside the A15. Irreversible damage is observed in all samples as soon as the intrinsic tensile region is approached. Even though the samples were less than perfect due to the exposed filaments in at least one of the samples (Fig. 1), this observation of crack formation around the maximum in the $I_c(\epsilon)$ behavior is consistent with recent literature results on high current RRP® wires [9].

IV. PARAMETRIZATION

The measured data are parameterized using the Twente Scaling Relation (TSR) [8]. The TSR, with variable pinning

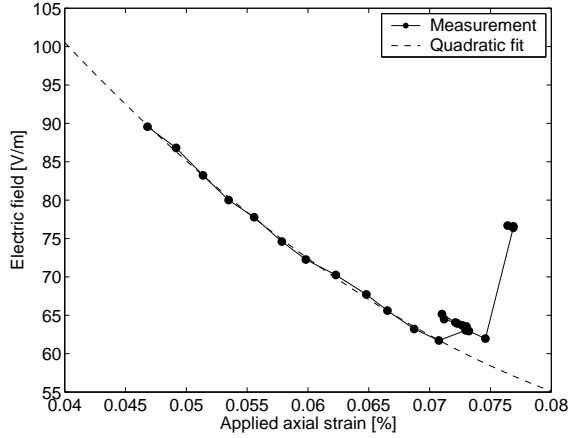


Fig. 4. Electric field as a function of applied axial strain at $\mu_0 H = 15$ T, $T = 4.21$ K and $I = 270$ A on sample 8781.

behavior (i.e. with p and q used as fit parameters), was recently accepted by the ITER community to replace the Summers relation [10]. It can be shown that the TSR can be mathematically simplified to [5]:

$$J_c(H, T, \epsilon) = \sqrt{2} C \mu_0 H_c^*(t) h^{p-1} (1-h)^q \quad (1)$$

with

$$\begin{aligned} H_c^*(t) &\cong H_c^*(0) (1-t^2), \\ t &\equiv \frac{T}{T_c^*(0, \epsilon)}, \quad h \equiv \frac{H}{H_{c2}^*(T, \epsilon)}, \\ T_c^*(0, \epsilon) &= T_{cm}^*(0) s(\epsilon)^{\frac{1}{3}}, \\ H_{c2}^*(T, \epsilon) &= H_{c2m}^*(0) MDG(t) s(\epsilon) \end{aligned}$$

The function $MDG(t)$ describes the shape of the field-temperature phase boundary and is defined as:

$$MDG(t) \equiv \frac{H_{c2}^*(t)_{MDG}}{H_{c2}^*(0)_{MDG}}, \quad (2)$$

in which $H_{c2}^*(t)_{MDG}$ and $H_{c2}^*(0)_{MDG}$ are solutions to the implicit Maki-De Gennes relation:

$$\ln(t) = \psi\left(\frac{1}{2}\right) - \psi\left(\frac{1}{2} + \frac{\hbar D^*(\epsilon) \mu_0 H_{c2}^*(T, \epsilon)}{2\phi_0 k_B T}\right). \quad (3)$$

$MDG(t)$ can be approximated by $(1-t^{1.52})$ to arrive at an explicit relation, but at the cost of errors in $H_{c2}^*(T, \epsilon)$ up to 0.4 T. For this reason we applied the implicit form in this work. The strain function $s(\epsilon)$ used here is the asymmetric deviatoric strain model, defined as:

$$\begin{aligned} s(\epsilon_a) &= \frac{1}{1 - C_{a1}\epsilon_{0,a}} \left(C_{a1} \left[\sqrt{(\epsilon_{sh})^2 + (\epsilon_{0,a})^2} \right. \right. \\ &\quad \left. \left. - \sqrt{(\epsilon_a - \epsilon_{sh})^2 + (\epsilon_{0,a})^2} \right] - C_{a2}\epsilon_a \right) + 1, \\ \epsilon_{sh} &= \frac{C_{a2}\epsilon_{0,a}}{\sqrt{(C_{a1})^2 - (C_{a2})^2}}, \\ \epsilon_a &= \epsilon_{applied} + \epsilon_m. \end{aligned} \quad (4)$$

For $C_{a2} = 0$, $s(\epsilon)$ reduces to the symmetric deviatoric strain model [4]. An improved model for the strain dependence of Nb_3Sn was recently proposed [11], but using the older form

allows for a more direct comparison with existing literature results. The definition of the parameters is extensively described elsewhere [8]. The TSR is available in the form of a spreadsheet, which can be downloaded from the internet [12].

Equation (1) is rewritten for the fits on critical current data in this publication, to provide a single pre-constant C_1 :

$$I_c(H, T, \epsilon) = C_1 (1-t^2) h^{p-1} (1-h)^q, \quad (5)$$

with $C_1 = \sqrt{2} C \mu_0 H_c(0)$.

V. RESULTS AND DISCUSSION

It was suggested elsewhere that a minimum data set to fully parameterize Nb_3Sn wires, consists of one $I_c(H)$ measurement at 4.2 K, one $I_c(H)$ at a sufficiently elevated temperature (e.g. 12 K), both at the same, unknown but constant strain state, and one $I_c(\epsilon)$ measurement at a convenient temperature and magnetic field [13]. It can be shown from (1) that this mathematically minimum required data set is indeed correct [5]. We therefore measured $I_c(\epsilon)$ at 4.21 K and 15 T and combined this with the $I_c(H, T)$ data (Fig. 2) and $I_c(H, T)$ verification measurements at $\epsilon_{applied} = -0.1\%$, -0.2% and -0.5% , to arrive at scaling parameters as summarized in Table II.

To account for the presence of inhomogeneities in the under-reacted wires, fits were made not only with $p = 0.5$ and $q = 2$, but also by using q as a fit parameter, since q is representative for the observable tails in Kramer plots (Fig. 2). It is seen from Table II, that the standard deviation σ does not significantly reduce, due to the fact that on samples 8781 and 9362 the tails were not measured. Also p was allowed to vary in a third fit, with only a slight reduction in σ as a result. This is reasonable, since no curvature was observed in the lower field region of the Kramer plots (Fig. 2), which is the region where p is effective. It is interesting to observe, however, that fitting p as well, causes the resulting values for H_{c2m}^* and C_1 to change significantly.

Inconsistencies are observed, if the effective field-temperature phase boundary that follows from a data fit with $p = 0.5$ and $q = 2$, is compared to the same phase boundary as calculated by linear extrapolation of the Kramer plots in Fig. 2. This inconsistency is graphically shown in Fig. 5 and represents an error in the temperature dependence in the TSR. The temperature dependence of H_{c2}^* is exact and unambiguously established ((3), [14]). Possible candidate errors, if (1) is assumed correct, are an incorrect temperature dependence of H_c or a need for an additional temperature dependence in the pinning description. The latter is arguably more likely, since specifically q can be expected to vary with temperature. q effectively fits the inhomogeneity averaging of H_{c2}^* over a range of compositions, and at different temperatures, this composition range over which the averaging occurs, varies. To what extent this reasoning is correct is subject to further research.

VI. COMPARISON WITH LITERATURE RESULTS

The obtained fits with $p = 0.5$ and $q = 2$ can be used to generate a calculated comparison with literature samples

TABLE II
SCALING PARAMETERS FOR SAMPLES 8781 AND 9362.

Sample	H_{c2m}^* [T]	T_c^* [K]	C_I [kA]	C_{a1}	C_{a2}	$\epsilon_{0,a}$ [%]	ϵ_m [%]	p	q	σ [A]
8781	27.0	16.7	1.66	43.4	0	0.14	-0.09	0.5	2	2.6
8781	26.6	16.7	1.62	43.2	0	0.14	-0.09	0.5	1.93	2.5
8781	29.1	16.7	3.77	43.8	0	0.16	-0.09	1.07	2.91	2.3
9362	26.4	15.9	1.07	43.0	0	0.23	-0.08	0.5	2	2.8
9362	25.6	15.9	1.04	42.6	0	0.22	-0.07	0.5	1.87	2.8
9362	29.0	15.9	2.10	43.2	0	0.28	-0.10	0.93	2.90	2.6

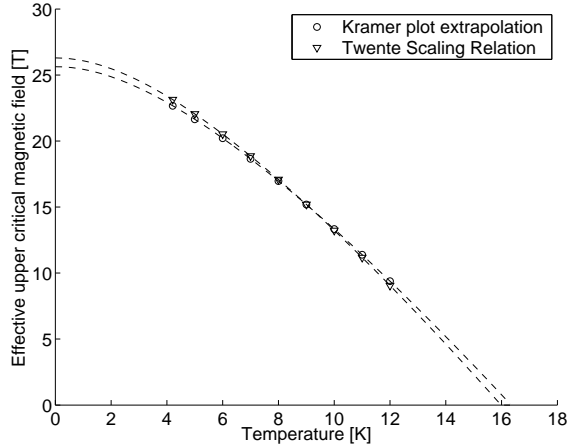


Fig. 5. Inconsistencies between the effective field-temperature phase boundary as calculated from the total I_c data fit and through linear Kramer extrapolation on sample 9362 at zero applied strain.

that were also analyzed using the TSR with $p = 0.5$ and $q = 2$, to analyze the strain sensitivity of high J_c RRP[®] wires relative to other wire types. A comparison like this can easily be calculated in terms of $I_c(\epsilon)$ at a constant temperature and magnetic field, which is the most relevant comparison for magnet applications. We leave this exercise to the enthusiastic reader. Such a comparison, however, will not account for differences in H_{c2}^* , which are known to result in differences in the strain dependence at constant magnetic field for e.g. ternary and binary wires of comparable layout [3].

A fair comparison of the *intrinsic* sensitivity to strain, has therefore to be normalized to H_{c2}^* , which means a comparison of the strain functions $s(\epsilon)$. Such a comparison is given in Fig. 6, using the scaling parameters from Table II (for $p = 0.5$ and $q = 2$), and literature parameters as summarized in Table III. It is found that the Powder-in-Tube (PIT) processed wires, and the literature high J_c RRP[®] wire exhibit favorable strain sensitivity. The Bronze processed wire exhibits an increased strain sensitivity, followed by the high J_c RRP[®] wires from the present measurements and the literature low loss, low J_c RRP[®] wire.

It should be emphasized that our present high J_c data are unreliable, due to the observation of exposed sub-elements, which could lead to local stress concentrations and therefore an *apparent* higher strain sensitivity.

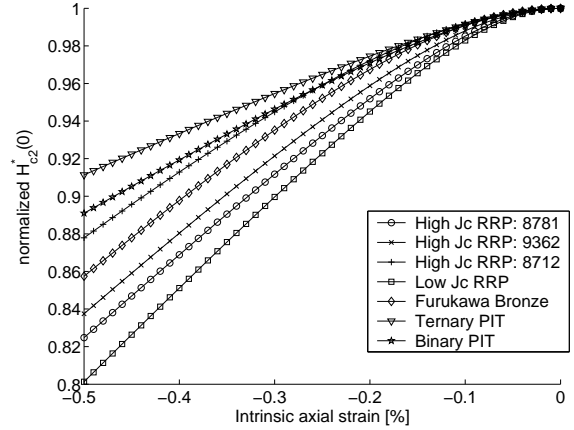


Fig. 6. Calculated comparisons of the axial strain function $s(\epsilon)$.

TABLE III
SCALING PARAMETERS OF LITERATURE SAMPLES.

Sample	H_{c2m}^* [T]	T_c^* [K]	C_{a1}	C_{a2}	$\epsilon_{0,a}$ [%]
High J_c RRP [®] 8712 [9]	29.3	15.9	59.4	23.9	0.31
Low J_c RRP [®] [15]	33.8	16.2	51.3	2.74	0.14
Ternary Bronze [8]	30.7	16.8	47.6	6.4	0.27
Binary PIT B36 [3]	24.2	17.0	64.1	36.1	0.17
Ternary PIT B105 [3]	29.3	17.0	58.1	36.3	0.12

VII. CONCLUSION

A new instrument to measure the critical current as a function of magnetic field, temperature, and axial strain, was successfully commissioned at LBNL. Various measurements have been performed on high J_c RRP[®] wire to demonstrate the instrument's capabilities. The initial results are hindered by sample mounting and soldering issues that will be resolved in future work. It is demonstrated how comparisons of the strain dependence of various wire types are easily accessible, once a commonly accepted scaling method is used, but the present strain dependence comparison is unreliable in terms of the samples described in this paper.

REFERENCES

- [1] A. Godeke, "A review of the properties of Nb₃Sn and their variation with A15 composition, morphology and strain state," *Supercond. Sci. and Techn.*, vol. 19, no. 8, p. R68, 2006.
- [2] D. R. Dietterich and A. Godeke, "Nb₃Sn research and development in the USA - Wires and cables," *Cryogenics*, vol. 48, p. 331, 2008.
- [3] A. Godeke, A. den Ouden, A. Nijhuis, and H. H. J. ten Kate, "State of the art Powder-in-Tube Niobium-Tin superconductors," *Cryogenics* 2008.

- [4] B. ten Haken, A. Godeke, and H. H. J. ten Kate, *J. Appl. Phys.*, vol. 85, p. 3247, 1999.
- [5] M. G. T. Mentink, "Critical surface parameterization of high J_c RRP Nb₃Sn strand," Lawrence Berkeley National Laboratory, Berkeley, CA, USA, Internship Report, 2008.
- [6] E. Barzi *et al.*, "RRP Nb₃Sn strand studies for LARP," *IEEE Trans. Appl. Supercond.*, vol. 17, no. 2, p. 2607, 2007.
- [7] A. Godeke *et al.*, "Experimental verification of the temperature and strain dependence of the critical properties in Nb₃Sn wires," *IEEE Trans. Appl. Supercond.*, vol. 11, no. 1, p. 1526, 2001.
- [8] A. Godeke, B. ten Haken, H. H. J. ten Kate, and D. C. Larbalestier, "A general scaling relation for the critical current density in Nb₃Sn wires," *Supercond. Sci. and Techn.*, vol. 19, p. R100, 2006.
- [9] A. Nijhuis, Y. Ilyin, and W. Abbas, "Axial and transverse stress-strain characterization of the EU dipole high current density Nb₃Sn strand," *Supercond. Sci. and Techn.*, vol. 21, p. 065001, 2008.
- [10] L. Bottura and B. Bordini, " $J_c(B, T, \varepsilon)$ parameterization for the ITER Nb₃Sn production," Paper 5LY06, presented at the 2008 Appl. Supercond. Conf., Chicago, IL, USA.
- [11] D. Arbelaez, A. Godeke, and S. O. Prestemon, "An improved model for the strain dependence of the superconducting properties of Nb₃Sn," Accepted for *Supercond. Sci. and Techn.*, 2008.
- [12] <http://www.magnet.fsu.edu/magnetechnology/research/asc/plots.html>.
- [13] A. Godeke, "Performance boundaries in Nb₃Sn superconductors," Ph.D. dissertation, Univ. of Twente, Enschede, The Netherlands, 2005.
- [14] A. Godeke *et al.*, "The upper critical field of filamentary Nb₃Sn conductors," *J. Appl. Phys.*, vol. 97, p. 093909, 2005.
- [15] Y. Ilyin, A. Nijhuis, and E. Krooshoop, "Scaling law for the strain dependence of the critical current in an advanced ITER Nb₃Sn strand," *Supercond. Sci. and Techn.*, vol. 20, no. 3, p. 186, 2007.